This is a repository copy of *Field statistics in an enclosure with an aperture: Effect of Q-factor and Number of Modes*.

Field Statistics in an Enclosure with an Aperture

Effect of Q-factor and Number of Modes

J F Dawson, T Konefal, M P Robinson, A C Marvin, S J Porter, L C Chirwa

Department of Electronics
University of York
York, England
jfdawson@iee.org

Abstract—**The statistics of the fields within an enclosure illuminated by an external field via an aperture have been investigated using Monte-Carlo methods. The field statistics in the volume of the enclosure are shown to correspond to the Rayleigh statistics found in properly functioning reverberation chambers when a sufficiently large number of modes is excited. The variation of field behaviour near the conducting walls is investigated. The deviation of the field statistics from the Rayleigh distribution as the number of excited modes falls is also investigated.**

Keywords - HIRF, reverberation chamber, shielding effectiveness, field statistics, enclosure, fuselage, mode-stir

I. INTRODUCTION

The determination of the shielding effectiveness (SE) of equipment enclosures and vehicle bodies (e.g. aircraft fuselage) is of significant interest to the EMC community. SE is usually defined as the ratio of (external) illuminating field to the internal field (at some point in the enclosure). However at frequencies where the enclosure is electrically large, the internal field magnitude can vary rapidly with position, frequency, and any small variations in geometry, rendering this measure ineffective. An understanding of the field statistics inside the cavity is therefore likely to provide a more useful measure of shielding. The results presented in this paper provide some insight into the behaviour of fields in electrically large enclosures that the authors believe will be of use in the understanding of shielding and EMC problems.

The behaviour of reverberation (mode-stirred) chambers is also of interest to the EMC community. Much work has already been done in this area to understand the behaviour of fields in electrically large enclosures. The analysis of field behaviour in reverberation chambers by Hill [1] and others [2] shows that under the ideal conditions of a large number of excited modes the probability density function of the magnitude of individual field components follows a Rayleigh distribution. The statistical behaviour of the field is independent of position in the cavity (assuming a sufficient distance from any conducting object - e.g. ~λ/4 from the walls). Arnaut [3] shows that the statistical behaviour of fields changes as the number of modes excited reduces. Here we show results of simulations that demonstrate these effects and

give a simple explanation of the phenomenon, which we hope will be of interest to those using reverberation chambers.

II. METHODOLOGY

A. Numerical methods

Three types of simulations were carried out in this paper:

- Matlab Monte-Carlo simulations using the known analytic modal field structures within an ideal enclosure – here we can artificially determine the number of modes excited with known amplitude and phase.

- Transmission-line Matrix (TLM) full-wave numerical field solutions for enclosures with apertures – these give realistic solutions of good accuracy but take considerable computer time.

- Intermediate Level Circuit Model (ILCM) simulations [4][5] for enclosures with apertures – these give a similar accuracy to the TLM model but run 3 orders of magnitude faster.

In the case of the TLM and ILCM models the Q-factor of the enclosure is controlled by adjusting the reflectivity of the wall opposite the aperture.

III. IDEAL ENCLOSURE

Our approach is initially to consider a single field component of a single resonant mode. We then generalise this to a multi-mode cavity where the modes are superposed with random phase differences, and may have different excitation coefficients. Finally we consider what happens when the points are constrained to be close to the cavity walls.

The statistical models all use the Monte Carlo method and are implemented in Matlab. A large number of positions (typically 10^5) are selected by choosing random values for the coordinates (x, y, z), and the electric field strength is calculated. A distribution or probability density function (PDF) is then constructed from the values of field strength. We have initially only considered the electric field, but the method is equally applicable to the magnetic field.

A. Single mode statistics

In this section we use Monte Carlo techniques to investigate the statistics of the electric field distribution inside a rectangular box. As reported in [1], we expect that the modulus of a single component of field is chi-distributed with two degrees of freedom (Rayleigh distributed), and has a probability distribution function (PDF) given by

$$P\big(|E_y|\big) = \frac{|E_y|}{\sigma^2} \exp\left[-\frac{|E_y|^2}{2\sigma^2}\right] \qquad (1)$$

Two conditions are generally agreed to be necessary to achieve the Rayleigh distributed pdf:

- that there are at least 60 resonant cavity modes possible below the frequency of interest [2];

- and that we are not too close to the cavity walls (at least a quarter of a wavelength away is often deemed to be sufficient).

For a single, transverse electric or transverse magnetic mode in a rectangular cavity the resonant frequency is given by

$$f_{mnp} = \frac{c_0}{2}\sqrt{\frac{m^2}{a^2} + \frac{n^2}{b^2} + \frac{p^2}{d^2}} \qquad (2)$$

where m, n and p are integers characterising the mode and a, b, d are the cavity dimensions. c_0 is the velocity of light in free space. At sufficiently high frequencies, nearly all the modes will have $n>1$, $m>1$ and $p>1$, and for such modes the normalised magnitude of the y-component of the electric field is given by:

$$E_y = \sin\frac{m\pi x}{a}\cos\frac{n\pi y}{b}\sin\frac{p\pi z}{d} \qquad (3)$$

There will be a standing wave pattern repeating along each of the three axes x, y and z. This means that the statistics of a 'unit cell' of this pattern will be the same as the statistics of the entire cavity. Therefore the statistical distribution can be found by considering the function

$$E(x,y,z) = \sin(\pi x)\sin(\pi y)\sin(\pi z) \qquad (4)$$

(the subscript 'y' has been dropped for convenience and the dimensions normalised) and choosing a large number of uniformly randomly distributed points in the range $0<x<1$, $0<y<1$, $0<z<1$. The substitution of a sine function for a cosine in Equation 4 does not alter the distribution. This distribution was evaluated using 10^5 points. Before considering the 3-d cavity we first considered the 1-d case:

$$E(x) = \sin\pi x \qquad (5)$$
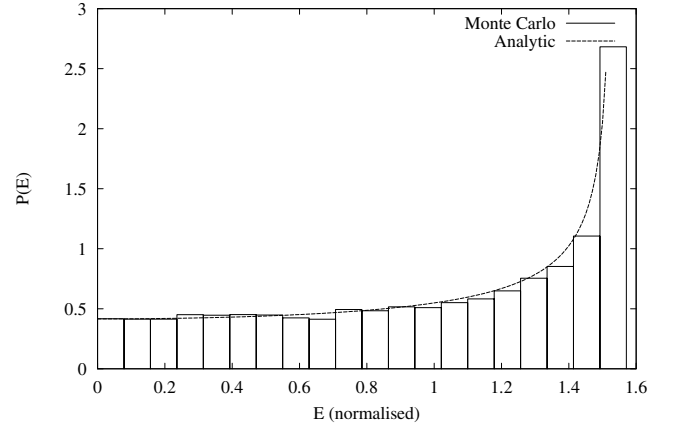
with the result shown in Figure 1.

Figure 1.   Statistical distribution of E-field for single mode, 1-d case
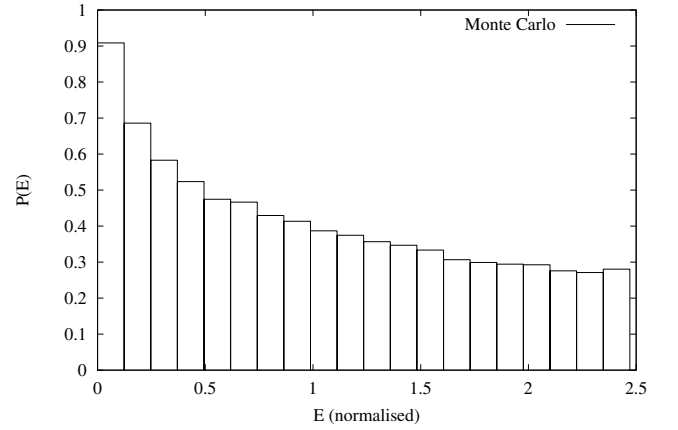

Figure 2.   Statistical distribution of E-field for single mode, 2-d case.

The result agrees with the analytical solution for the PDF of a sine wave,

$$P(x) = \frac{2}{\pi\sqrt{1-x^2}} \qquad (6)$$

where $x = E/E_{max}$, giving us confidence in our method. We then considered the 2-d and 3-d cases.

The results for the full 3-d case (Equation 4) is shown in Figure 3. The shape of this distribution can be explained by the fact that there are only a few points near the centre of the unit cell that have values of $E \approx 1$, but there are many points near the edges of the unit cell that have values of $E \approx 0$. It is interesting to compare the 3-d and 1-d distributions (Figure 3. and Figure 1.).
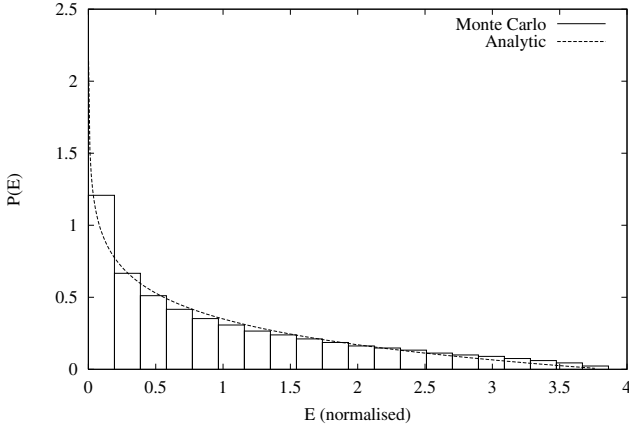
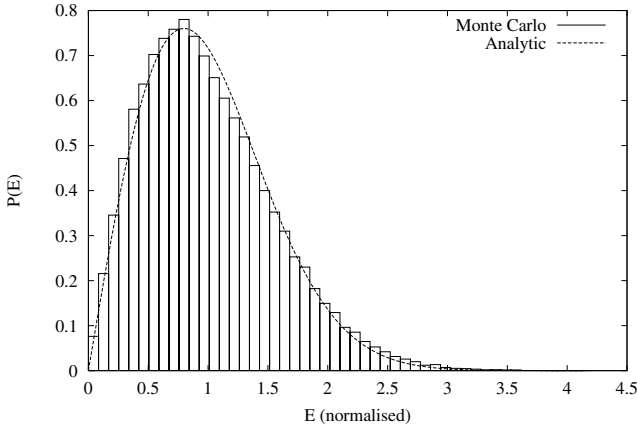Figure 3. Statistical distribution of E-field for single mode, 3-d case

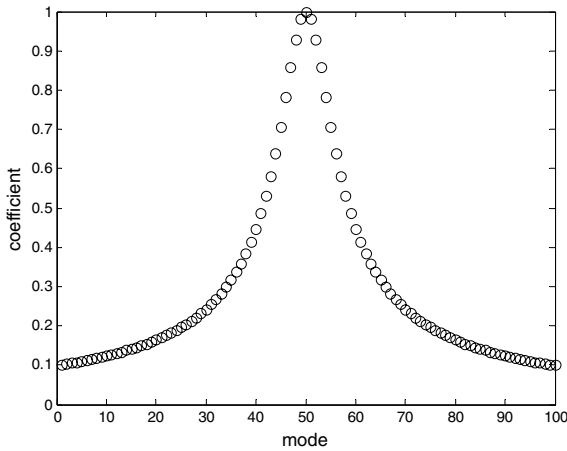Figure 4. Statistical distribution of E-field for ten modes, 3-d case, equal mode coefficients

Figure 5. Lorentzian distribution of mode coefficients for α=10.

B. Multi-mode statistics

In a real cavity at high frequency, several modes will all be excited simultaneously. Our first model for multi-mode statistics took a number of modes each with distributions of the type shown in Figure 3. and combined them with random phase differences:

$$E_T = \left| \sum_i c_i E_i \exp(-j\zeta_i) \right| \qquad (7)$$

Here ζ_i was chosen randomly in the range $0 \le \zeta_i < 2\pi$, E_i is calculated as in Equation 3, and the subscript i represents a distinct (m, n, p) triplet. Initially all the coefficients c_i were made equal to unity. It was found that with 10 or more modes, the combined distribution was similar to the Rayleigh distribution,

$$p(E) = \frac{E}{\sigma^2} \exp\left(\frac{-E^2}{2\sigma^2} \right) \qquad (8)$$

An example is shown in Figure 4. For fewer than 10 modes the distribution had a form intermediate between the mono-mode distribution of Figure 3. and the Rayleigh distribution.

We then refined our model to account for the fact that the mode coefficients c_i should depend on the difference between the resonant frequency of the mode and the excitation frequency. The further away from the peak, the lower the coefficient. The standard theory of a simple oscillator shows that the frequency response of each mode should follow a Lorentzian curve. If we assume that the modes are uniformly spaced (in the frequency domain) with mode density d_m (in modes/Hz), and the excitation frequency f_0 corresponds to the resonant frequency of a mode i_{max}, then we can derive a formula for the mode coefficients:

$$c_i = \frac{\alpha}{\sqrt{4(i - i_{max})^2 + \alpha^2}} \qquad (9)$$

where

$$\alpha = \frac{f_0 d_m}{Q} = f_{bw} d_m \qquad (10)$$

α is the product of mode density d_m and 3-dB bandwidth f_{bw}. This function is shown in Figure 5. and Figure 6. for α=10 and α=0.1.
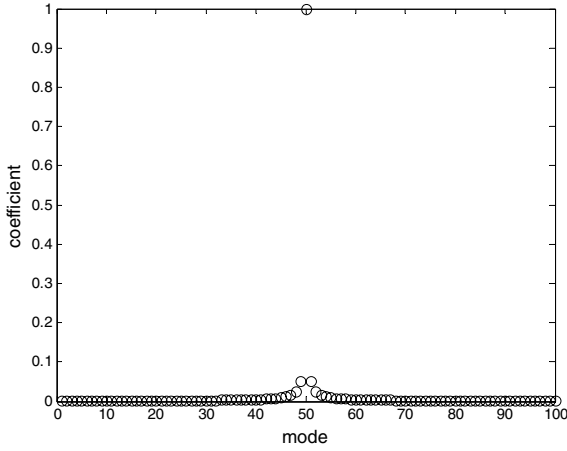
Figure 6.   Lorentzian distribution of mode coefficients for α=0.1

It was found that for α>1 the distribution of ET in Equation 7 was similar to the Rayleigh distribution, but that for values less than one the distribution became more like the mono-mode distribution of Figure 3. The results for values of α varying from 0.1 to 30 are compared in Figure 7. A physical explanation for this behaviour is that as the modes become closer together (or the bandwidth increases), more and more modes are coupled to the excitation frequency, and the distribution shifts from 'mono-mode' to 'Rayleigh.'

C.   Field statistics near the cavity walls

Research into stirred-mode chambers has suggested that provided a sufficiently large number of modes are present, the statistical distribution of a field component near the centre of the chamber should follow the Rayleigh distribution.   To qualify this statement more precisely, it is widely held that Rayleigh statistics apply provided that the distance from the walls (or any other conducting structure) is greater than one quarter of the free-space wavelength.

To test the validity of this 'quarter wave rule' we used Monte Carlo techniques to investigate the variation of statistical distribution with position in a cavity. We modelled the screened room in our EMC Laboratory at York, because we are very familiar with its resonant properties. The dimensions of this room are $4.70 \times 3.00 \times 2.37$m, and the fundamental resonant frequency is 59MHz.

In our model we first evaluated all the TE resonances of the screened room up to a frequency of 2GHz. We selected the first thirty modes that have a resonant frequency of greater than 1GHz. To combine the modes we added the field strengths E_i with equal coefficients c_i and random phase differences ζ_i, as in Equation 7. To find the y-components for each of the thirty modes, we used Equation 3 with appropriate values of m, n and p for the particular mode. However, rather than choosing random values for x, y, and z, we constrained x to be a fixed value and varied y and z only. The values were chosen to be x=1.5m (mid-way across the room), x=0.15m (a half-wavelength from the wall) x=0.075m (quarter wavelength) and x=0.0375m (eighth of a wavelength).   The resulting field distributions at different distances from the side walls are

compared in Figure 8. .   Note that the distribution still resembles a 'Rayleigh' distribution when the distance is less than a quarter wavelength, but that the most probable field is reduced in value.
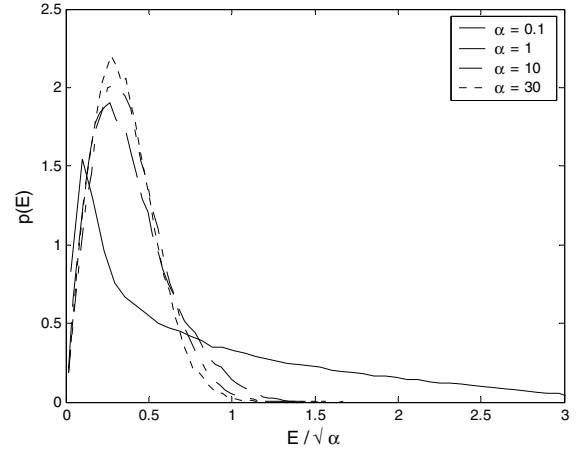

Figure 7.   Multi-mode statistical distributions for various values of α.
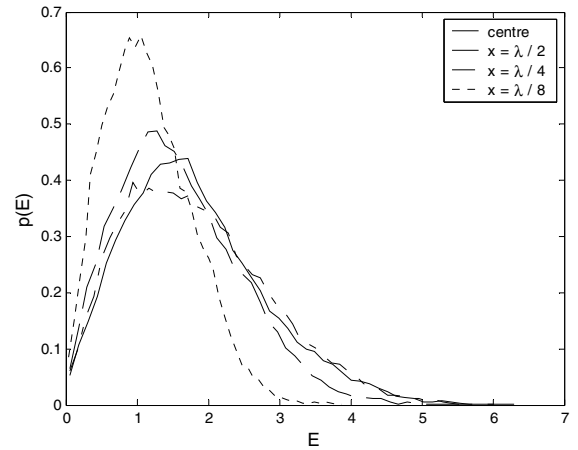

Figure 8.   Distribution of vertical E-field for different horizontal positions

To investigate this phenomenon further we calculated the statistics for a large number of horizontal positions and plotted the mean value of E_y against x. The results are shown in Figure 9. on a logarithmic scale. It can be seen that this model confirms the quarter-wave rule for the screened room. The fluctuations in E_y at $x>\lambda/4$ appear to vary randomly if the frequency is slightly changed, but the fall of E_y for $x<\lambda/4$ is repeatable.   An explanation for this behaviour is that the boundary conditions constrain the tangential field component to be zero at the side walls for all of the contributory modes.

A similar model was constructed but this time we constrained the value of y and randomised x and z. The results are shown in Figure 10. It can be seen that when the vertical distance from the floor (or ceiling) of the room becomes less than a quarter wavelength, the mean vertical field now *increases*. Again this can be explained by the boundary conditions which now apply to a normal electric field rather

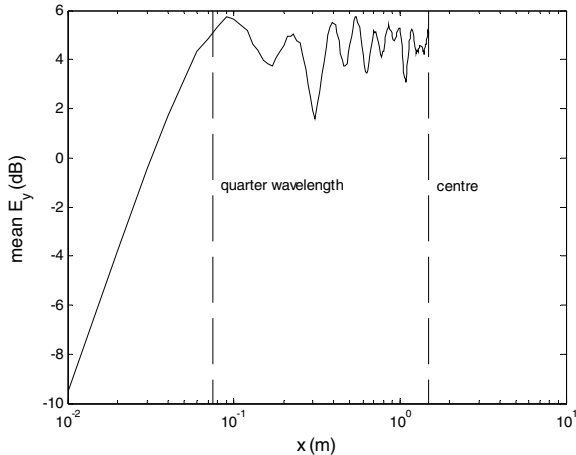than a tangential field. The above models confirm the quarter-wave rule.

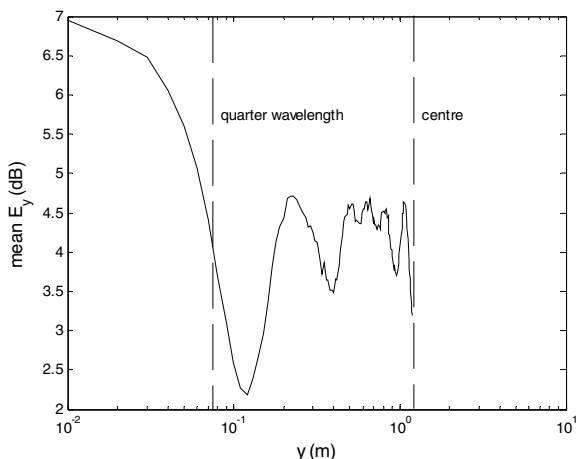Figure 9.   Variation of mean vertical E-field with horizontal position

Figure 10. Variation of mean vertical E-field with vertical position

D. *Enclosures with an aperture*

Initially, we consider a rectangular box of size 60cm(x)×30cm(y)×90cm(z) with a rectangular aperture of size 8cm×1cm, asymmetrically positioned in the front face of the box (the plane $z=0$). Ten thousand randomly selected points within the back half of the box (i.e. well away from the aperture) were used to sample the field $|E_y|$ as calculated using an ILCM model. A frequency of 2999.7MHz ($\approx$3GHz) was chosen, which requires consideration of TE$_{mn}$ and TM$_{mn}$ modes up to $m_{max} = 13$, $n_{max} = 7$, in order to include all propagating modes below and up to 3GHz. Indeed, many evanescent modes are also included in this choice of m_{max} and n_{max}, which covers 195 modes in total, excluding TE$_{0n}$ modes. The TE$_{0n}$ modes are ignored because the field E_x along the length of the slot is assumed to be zero, since the slot is assumed to support a TEM wave with no longitudinal component. TE$_{0n}$ modes are thus not excited by the aperture

field. In selecting the 10,000 random positions within the box at which to sample $|E_y|$, we deliberately keep at least 3cm from the walls of the cavity, in order to fulfil the condition that we are at least a quarter of a wavelength (2.5cm at 3GHz) from the walls. Below 3GHz there are approximately 1339 resonant modes as calculated from [6]. This is well above the generally accepted minimum number of modes (60) required for a Rayleigh distribution for $|E_y|$.   Having fulfilled the two conditions set in Section A therefore, it was anticipated that the model would predict a Rayleigh distribution for the field $|E_y|$. Figure 11. shows the distribution computed from the model for the field $|E_y|$, which is clearly not a Rayleigh distribution. Instead, the distribution appears to be somewhere between the monomode distribution of Figure 3. and the Rayleigh distribution of Figure 4. In fact, the distribution is unaltered even if we include random positions near (but at least 3cm away from) the aperture itself.

It is instructive to compare the PDF of Figure 11. with an approximate single mode model. For the box modelled in Figure 11. , there is a resonant mode at frequency $f_{mnp} = 3.00\text{GHz}$, as calculated from Equation 2 with $m = 12$, $n = 0$ and $p = 1$. If this mode were to dominate the field pattern within the box at 2999.7MHz, we would expect the field E_y to be largely determined by the distribution given in Equation 3 with $m = 12$, $n = 0$ and $p = 1$. The PDF for the (predominantly) monomode case with $n = 0$ is given approximately [7] by:

$$p(E_y) = -\frac{1}{E_{max}} \ln\left(\frac{E_y}{E_{max}}\right) \qquad (11)$$

This function is compared with the ILCM prediction in Figure 11. Although the agreement is reasonable, it must be borne in mind that there are many resonant modes in the box at about 3.0GHz (e.g $\pm15\text{MHz}$), some with $n = 0$ (about 7 modes) and some with $n \neq 0$ (about 18 modes). Depending on the Q of the resonances, it is likely that the ILCM model is encompassing several modes to a greater or lesser extent. In fact, though no details are given here, a detailed Fourier decomposition of the cavity field shows that there are 3 modes within a 10dB bandwidth of the maximum modal amplitude. This is consistent with a PDF intermediate between the mono-mode distribution of Figure 3. and the multimode Rayleigh distribution of Figure 4. , as indicated in Section B. Indeed, when the Q of the box is reduced sufficiently by making the back wall in the ILCM partially absorbing with a reflection coefficient of $\rho = -0.5$, the field $|E_y|$ is found to follow the Rayleigh distribution as in Figure 12. . This is consistent with the Monte-Carlo modelling of Section B, where reducing Q in Equation 10 increases α above unity and the distribution

changes from 'mono-mode' to 'Rayleigh.' The result is repeatable using TLM, also indicated in Figure 12. (the TLM results were scaled to give the same mean field here in order to better illustrate the shape of the distribution). Fourier decomposition of the Rayleigh-like ILCM results here shows that there are 13 modes within a 6dB bandwidth of the maximum amplitude, again consistent with the Monte-Carlo results of Section B.
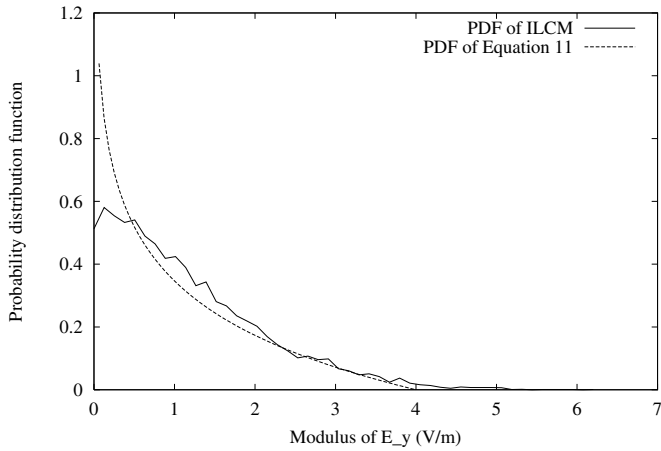

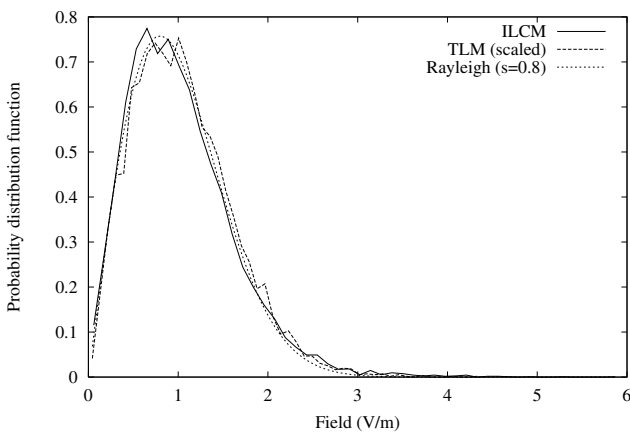Figure 11. Qualitative 2-d analysis of ILCM model results with dominant TE$_{m0}$ modes.

Figure 12. PDF of $|E_y|$ at 2999.7MHz with a back wall reflection coefficient of $\rho = -0.50$, compared with a Rayleigh distribution with $\sigma = 0.75$.

We were also concerned that the presence of the aperture as a source of energy would alter the field statistics. Figure 13. uses the same ILCM data as Figure 12. , but shows the PDFs of the field in the front half on the enclosure near the slot, along with the PDF in the rear half of the enclosure, away from the slot), and the PDF for the complete enclosure. It can be seen that there is a small difference in the field statistics.

IV. CONCLUSIONS

We have shown that the field statistics in an enclosure only take the form of a Rayleigh distribution when the ratio of mode

bandwidth to mode density, α, is significantly larger than one and gradually reduces to the single mode PDF when α falls below one. We have demonstrated that the tangential electric field mean-amplitude decays to zero as a conducting wall is approached starting approximately one-quarter wavelength from the wall. Also that the normal electric field component increases to approximately twice the value in the volume of the room, as a conducting wall is approached. This confirms the rule commonly used in reverberation chambers that the fields can only be considered uniform at a distance of greater than one quarter wavelength from any conducting surface..
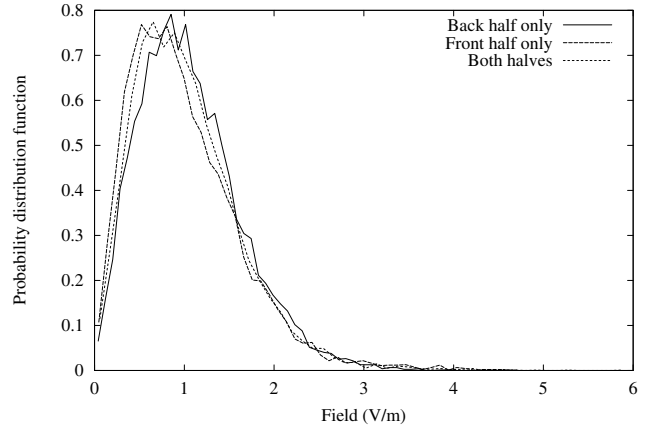

Figure 13. PDF of $|E_y|$ at 2999.7MHz with a back wall reflection coefficient of $\rho = -0.50$, comparing field in half of box near slot with back half.

REFERENCES

[1] D A Hill, Electromagnetic Theory of Reverberation Chambers, NIST technical note 1506, December, 1998

[2] P. Corona, J. Ladbury, and G. Latmiral., "Reverberation-chamber research-then and now: a review of early work and comparison with current understanding", IEEE Transactions on Electromagnetic Compatibility, 44(1):87-94, February 2002.

[3] L. R. Arnaut, "Compound exponential distributions for undermoded reverberation chambers", IEEE Transactions on Electromagnetic Compatibility, 44(3): 442-457, August 2002.

[4] J. F Dawson, T. Konefal, A. C. Marvin, S. J. Porter, M. P. Robinson, C Christopoulos, D W P Thomas, A Denton, T. M. Benson, "Intermediate level tools for Emissions and Immunity: Enclosure contents to Aperture coupling", IEEE International symposium on EMC , pp. 183-188, 13-17 Aug. 2001, ISBN 0-7803-6569-0

[5] I D Flintoft, N L Whyman, J F Dawson and T Konefal, "A Fast and Accurate Intermediate Level Modelling Approach for Electromagnetic Compatibility Analysis of Enclosures", IEE Proceedings on Science, Measurement and Technology, Special Issue on Computational Electromagnetics, Vol. 149, No. 5, September 2002, pp. 281-285.

[6] Liu, B.H., Chang, D.C. and Ma, M.T., "Eigenmodes and the composite quality factor of a reverberating chamber," National Bureau of Standards, Technical Note 1066, 1983

[7] T. Konefal, "Development of intermediate level modelling tools", Ninth quarterly report for BAE Systems, Electronics Department, York University, February 2004